Characterization of early 20th-century German bandstands metal alloys exposed to the Amazonian weathering of Belém, Brazil

Caracterização das ligas metálicas de coretos alemães do início do século XX expostos ao clima amazónico de Belém, Brasil

THAINÁ THAIS SILVA OLIVEIRA [1*] (ID)

FLÁVIA OLEGÁRIO PALÁCIOS [1,2] (ID)

1. Federal University of Pará, Cultural Heritage Sciences Graduate Program, Architecture and Urban Planning Graduate Program, Castilhos França Blvd. (w/o no.), 66010-060 Belém, Pará, Brazil

2. Federal University of Pará, Conservation and Restoration Faculty, Castilhos França Blvd. (w/o no.), 66010-060 Belém, Pará, Brazil

thainatsoliveira@gmail.com

Abstract

The iron industry's progress in the 18th and 19th centuries has left a noteworthy built heritage in non-European countries, such as Brazil. Among the cities, Belém holds five metallic bandstands imported from Germany and installed in Batista Campos Square in 1903. Despite the historical, architectural, technical, and social significance, these structures are facing gradual deterioration, disfigurement, and improper maintenance due to a lack of knowledge. To address these issues and gain a deeper understanding of the materials, this paper aims to characterize the metal alloys and corrosion products of these bandstands. Scanning electron microscopy, energy dispersive X-ray spectroscopy, and X-ray diffraction analyses were conducted on different structural parts. The results showed a significant use of nodular gray cast iron, steel application, their corrosion products, and an assessment of the conservation state of the coatings. This information enhances the knowledge of the use of ferrous alloys and their corrosion in historical buildings.

KEYWORDS

Iron alloys
Cast iron
Corrosion products
Iron architecture
Architectural heritage

Resumo

O progresso da indústria do ferro nos séculos XVIII e XIX deixou um património edificado notável em países não europeus, como o Brasil. Em particular, a cidade de Belém possui cinco coretos metálicos importados da Alemanha e instalados na Praça Batista Campos, em 1903. Apesar do seu significado histórico, arquitetónico, técnico e social, estes coretos estão sujeitos a uma gradual deterioração, descaracterização e ações de manutenção inadequadas resultantes da falta de conhecimento. Este artigo pretende caracterizar as ligas metálicas e os produtos de corrosão destes coretos. Foram realizadas análises por microscopia eletrónica de varrimento, espectroscopia de raios X por dispersão em energia e difração de raios X em diferentes componentes construtivos. Os resultados mostraram o uso abundante de ferro fundido cinza nodular, a aplicação de aço, o tipo de corrosão e o estado de conservação dos revestimentos. Essas informações ampliam o conhecimento sobre a utilização de ligas ferrosas e sua corrosão em edifícios históricos.

PALAVRAS-CHAVE

Ligas de ferro
Ferro fundido
Produtos de corrosão
Arquitetura do ferro
Património arquitetónico

Introduction

Different alloys, particularly ferrous ones, form part of the material fabric of the world's built cultural heritage. A significant portion of this legacy directly stems from historical events that unfolded in Europe during the eighteenth and nineteenth centuries, culminating in the advancement of the iron industry and the Industrial Revolution. As a result of these developments, several European nations manufactured and exported metallurgical and architectural products to other continents, including prefabricated iron buildings from 1840 onwards [1-2].

Buildings of this type, in which iron alloys were used as the main structural and constructive material and exposed means of aesthetic expression, were referred to as "iron architecture" [2-3]. Many Latin American countries, particularly Brazil, were major importers of this style. Belém, located in the Amazonian region of Brazil, stands out among the cities with the most important collections dating from the nineteenth and twentieth centuries. Among markets, chalets, pavilions, and street furniture, the city has a significant set of bandstands [2, 4].

The bandstands were imported during a period of intense economic growth driven by rubber exports. The surplus of wealth spurred an extensive redevelopment of the city's central urban area, focusing on the remodeling and creation of parks and squares [5-6]. According to official reports by Antônio Lemos [7], the city's intendant (1897-1910) and key figure in leading much of the transformation during this period, five musical pavilions of German origin were ordered in 1903 to be installed at the Batista Campos Square (Figure 1a-b).
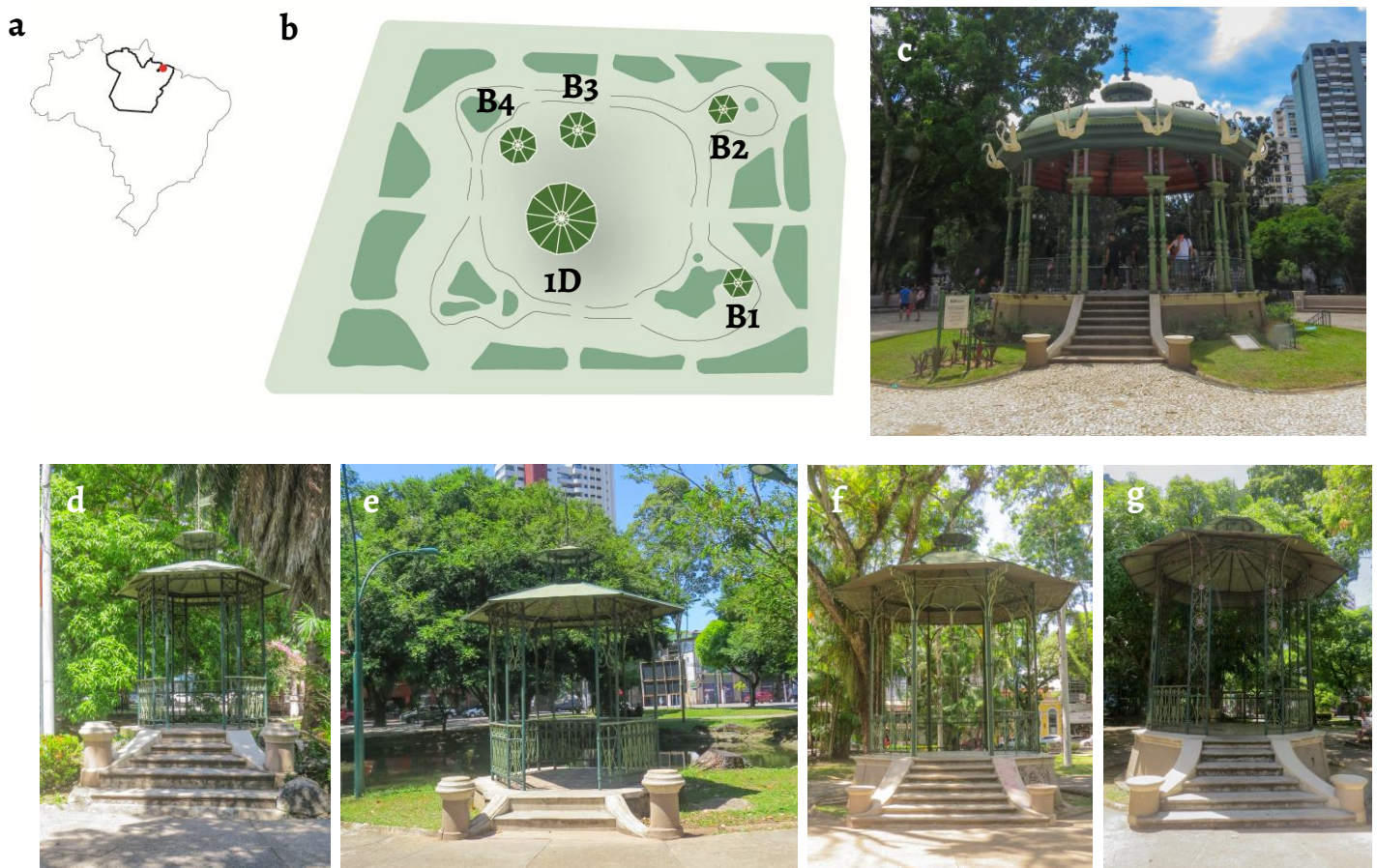

Figure 1. Musical pavilions of German origin: *a)* Location of the German bandstands within the Brazilian territory; *b)* the boundaries of the square; *c)* The Primeiro de Dezembro Pavilion; *d)* Bandstand 1; *e)* Bandstand 2; *f)* Bandstand 3; *g)* Bandstand 4.

Even though these structures vary in size, they share numerous architectural and stylistic features, supporting the theory that they originated from the same manufacturer [8]. The largest structure, located in the center of the square, is called the *Primeiro de Dezembro Pavilion* (Figure 1c). The other four, which are small to medium in size, are distributed throughout the park: Bandstands 1, 2, 3, and 4 (Figure 1d-g).

After more than a century, these structures have been listed as part of historical sites. Despite their significance, our understanding of them remains insufficient to address issues such as degradation and architectural disfigurement. These issues escalated in 2020/2021, when their severely decaying state demanded an intervention that primarily prioritized paint renovation. The maintenance of paints for metals is undoubtedly fundamental for protection and aesthetics [9]. However, the lack of information is especially pronounced when it comes to the detailed identification of their physical, chemical, and mineralogical characteristics through scientific methods. This missing knowledge is essential for guiding other appropriate conservation and restoration strategies, as well as for assessing the extent of deterioration.

It is also important to note that each country developed its own standards until the early twentieth century, resulting in a wide range of ferrous metals with heterogeneous properties [10]. There are still indications that knowledge was not shared between foundries [11]. Since the bandstands represent the technological development of an era, the study of these structures addresses broader issues beyond local context preservation. Both objective and subjective insights are expected to contribute to the history of technology and construction and to deepen the understanding of the global industrial heritage.

Given these considerations, this research aims to characterize the metallic alloys and corrosion products of Belém's German bandstands, located at Batista Campos Square, using analytical techniques. This investigation is crucial for the conservation and restoration of historical metals, as it provides evidence-based data and a solid foundation for defining conservation treatments [12-13]. Therefore, it serves as both a basis for restoration actions on the buildings themselves and as documentation of structures and construction technologies affected by the Amazonian weathering.

Materials and methods

Sampling

The samples come from the five buildings located at the Batista Campos Square: The Primeiro de Dezembro Pavilion and Bandstands 1, 2, 3, and 4. Since they are listed heritage, the sampling procedure was carefully conducted and authorized by Pará's Historical, Artistic, and Cultural Heritage Department (DPHAC)/Culture Department (SECULT) and Belém's Design and Landscaping Department (DPP)/ Environment Department (SEMMA).

Considering them as legally protected and recently restored buildings (2020/2021), the number of samples was restricted as much as the areas allowed for extraction. Small fragments, up to 2 cm, were collected from parts affected by gaps or crevices so that additional further damage was not caused. Even so, constructive representativity was ensured since different parts of the bandstands could be sampled. In total, nine samples from various architectural elements – such as roof sheet, pillar, guardrail, and ornament – were analyzed.

The collected materials included metal alloy, corrosion products, and coating samples. It should be noted that the presence of coatings was an incidental finding from the sampling process and not the primary focus of the investigation because they were new. Nonetheless, they were considered in this study for their important role in corrosion protection or progression. These samples are described in Table 1, and their locations and typical visual aspects are illustrated in Figure 2.

For historical metals, analytical techniques can be used to obtain crucial data through the microstructural and chemical characterization of the metallic substrate and corrosion products

[12-13]. On this subject, scanning electron microscopy and energy dispersive X-ray spectroscopy (SEM/EDS) are fit to observe these features. X-ray diffraction can additionally identify crystalline phases for mineralogical insights. Overall, they can provide information about manufacturing procedures and deterioration processes.

Table 1. Identification of the samples according to the building, area, type, and analytical technique used for the material characterization.

| Building	Sample	Sampling area	Type of sample	Analytical technique
Primeiro de Dezembro Pavilion	1D-A1	Guardrail	Metal alloy, corrosion prod. & coating	SEM-EDS
	1D-A3	Roof sheet	Metal alloy, corrosion prod. & coating	SEM-EDS
	1D-A4	Roof sheet	Metal alloy	XRD
Bandstand 1	B1-A2	Guardrail	Metal alloy	XRD
	B1-A4	Guardrail	Metal alloy, corrosion prod. & coating	SEM-EDS
Bandstand 2	B2-A1	Ornament	Metal alloy	XRD
	B2-A4	Pillar	Metal alloy, corrosion prod. & coating	SEM-EDS
Bandstand 3	B3-A3	Pillar	Metal alloy, corrosion prod. & coating	SEM-EDS
			Metal alloy	XRD
Bandstand 4	B4-A4	Pillar	Metal alloy, corrosion prod. & coating	SEM-EDS
			Metal alloy	XRD
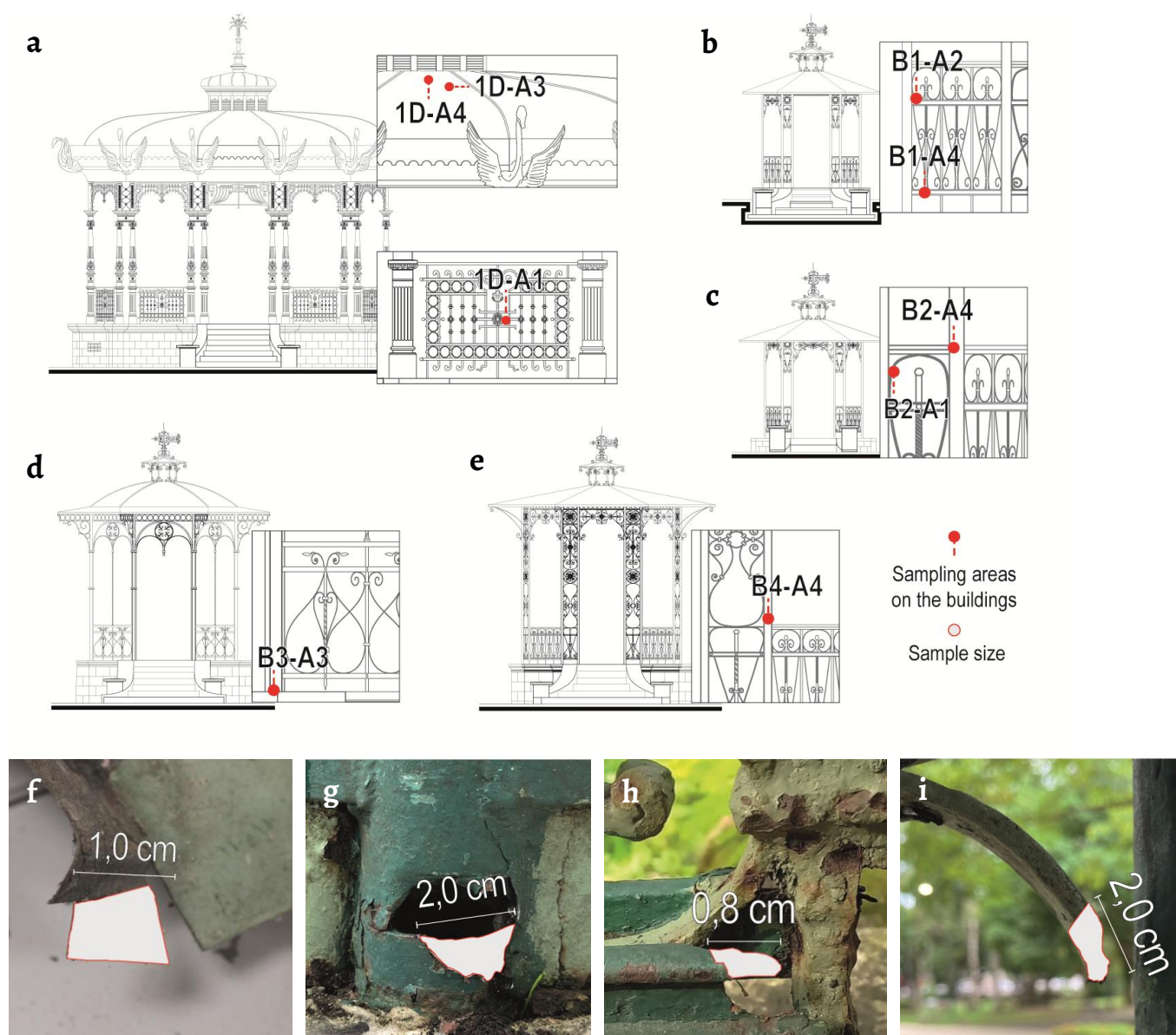
Figure 2. The sampling areas: *a)* Primeiro de Dezembro Pavilion; *b)* Bandstand 1; *c)* Bandstand 2; *d)* Bandstand 3; *e)* Bandstand 4; Examples of the covered architectural elements, areas, and sizes: *f)* roof sheet; *g)* pillar; *h)* guardrail; *i)* ornament.

Analytical techniques

The physical characterization was performed by scanning electron microscopy (SEM), combined with energy dispersive X-ray spectroscopy (EDS) for chemical element identification at selected spots. The microscope used was a Hitachi brand, TM3000 model, capable of magnifications up to 30,000× operated with acceleration voltage from 5 or 15 kV beams. EDS spectra were obtained using an Oxford Instruments brand, SwifitED300 model X-ray dispersive energy spectrometer, which detects elements from boron (B_5) to Uranium (U_{92}). The images and elemental analyses were obtained at an acceleration voltage of 15 kV and with an acquisition time of 40 s.

The samples were observed in cross-section using SEM-EDS to determine the boundaries of the layers: metallic substrate, corrosion products, and coatings. They were first embedded in polyester mounting resin and then polished. Manual thinning was performed with wet sandpaper of different grit sizes: 100, 200, 400, 600, 1200, and 1500. Final polishing was achieved using 1/4 µm metallographic diamond paste and velvet discs.

The mineralogical composition of the alloys was analyzed by X-ray diffraction (XRD) with a BrukerD2 PHASER model diffractometer. The analyses used a Cu Kα radiation (1.54184 Å), at 300 W (30 kV and 10 mA). Data were collected in the 2θ range from 5° to 75°, with a step size of 0.02° and a step time of 0.2 s. Phase identification was performed using PANalytical X'Pert High Score Plus software. In this study, its application was reserved for the alloys due to the availability of samples previously explained.

Because of the limited volume available of the samples, micropreparation was used for the XRD analyses. The samples were manually ground using an agate mortar and then transferred to silicon plates (zero background).

All mentioned equipment belongs to the Mineralogy, Geochemistry, and Applications Laboratory (LAMIGA) of the Geosciences Institute of the Federal University of Pará (UFPA).

Results

General characteristics of the sampling

Based on the SEM cross-sectional images, the nine samples exhibit two main physical characteristics related to texture, which initially separates them into two groups: 1) uncorroded metallic substrate and 2) corrosion products, as indicated in Figure 3. The first group consists of samples with a solid and homogeneous matrix. The second group, in contrast, displays less consistency caused by corrosion and forms a layer in immediate contact with the unaltered alloy. The groups also differ chemically, as indicated by the grayscale colors reflecting the contrast in atomic numbers of the elements observed through the backscattered electron mode of the SEM [14].

The EDS spectra confirmed that the chemical composition of the unaltered metal is primarily iron. Some points also revealed smaller amounts of other elements such as carbon, manganese, silicon, sulfur, and phosphorus (Figure 3). The diffractogram in Figure 3 supports these findings, pointing ferrite (α-Fe, pure iron) as the predominant mineral phase [15]. Additionally, the B3-A3 sample exhibited an extremely low copper peak in its mineralogical composition. The only exception was in sample 1D-A4, where only zinc was identified by XRD (Figure 4).

The chemical composition of the unaltered areas is consistent with cast iron alloys, specifically the gray cast iron. The appropriate concentrations of carbon, silicon, and phosphorus promote graphite formation, leading to the production of gray cast iron. Although manganese and sulfur have opposing effects compared to the elements mentioned above, they still play a crucial role in forming manganese sulfide (MnS) which neutralizes the effects of sulfur – usually originating from natural sources – thereby preventing undesirable effects such as material weakening [16-18].
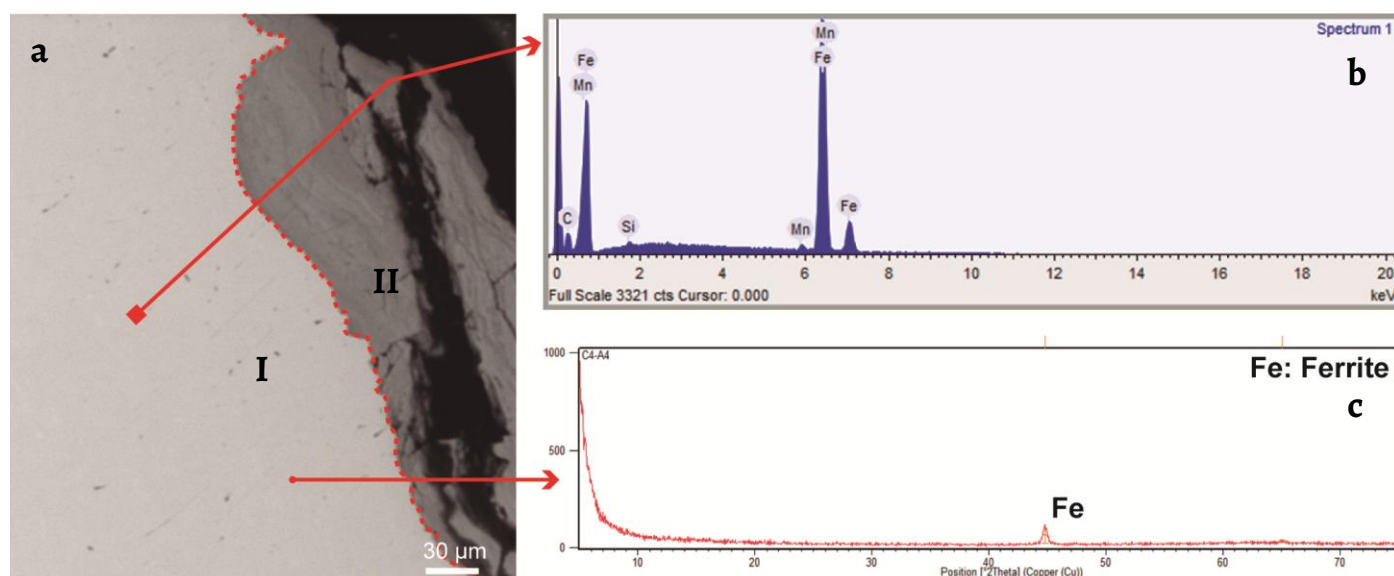
Figure 3. Sample B4-A4: *a)* SEM image indicating the boundary between the I) uncorroded metallic substrate and II) corrosion product layer; *b)* EDS spectrum; *c)* X-ray diffractogram, showing its chemical and mineralogical characterization.
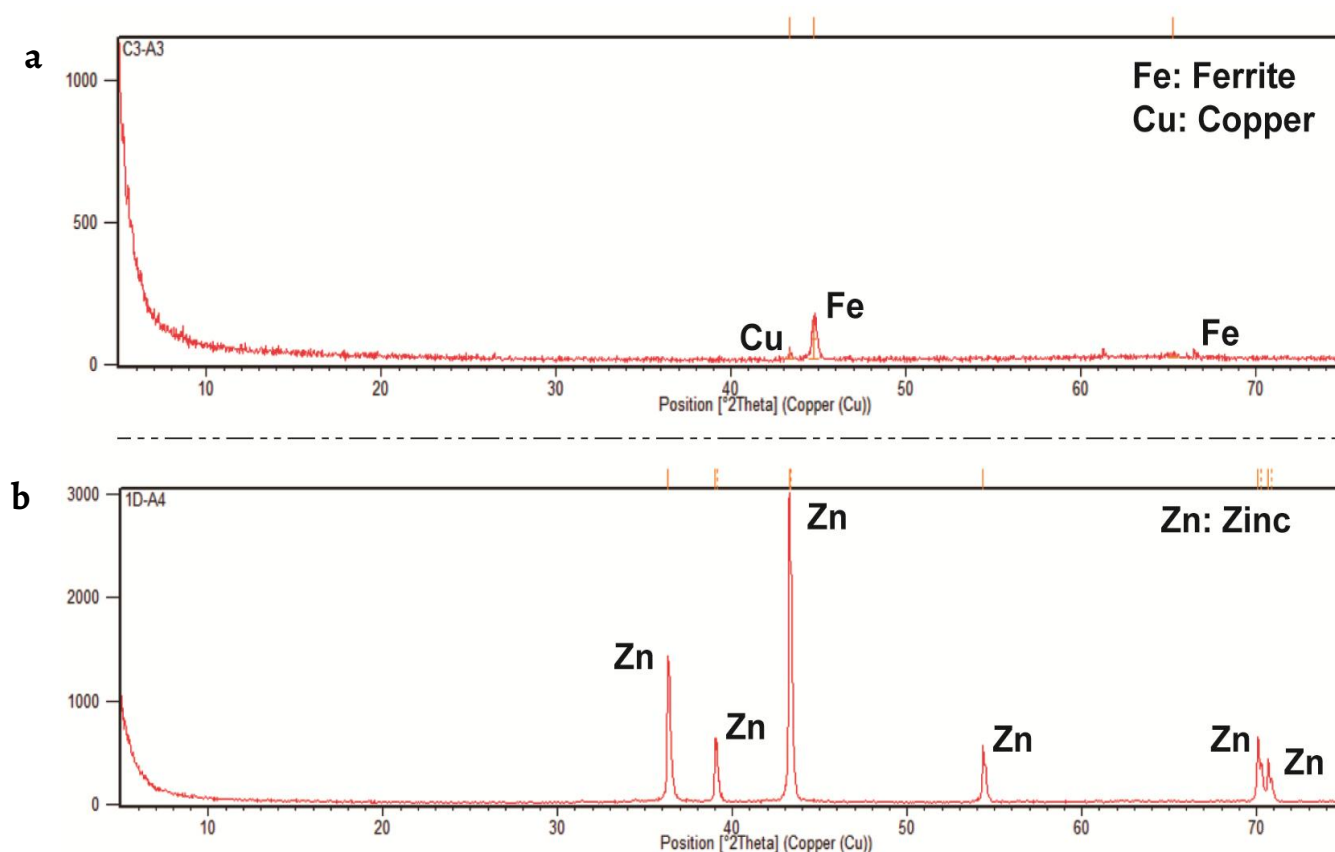

Figure 4. X-ray diffractograms: *a)* sample B3-A3 showing Fe and Cu; *b)* sample 1D-A4 showing Zn.

As expected, the corrosion products show a wider composition common to structures exposed to outdoor atmospheric corrosion. In addition to typical cast iron alloying elements, sodium, calcium, potassium, chlorine, aluminum, zinc, and bromine were also identified. These can be attributed to extrinsic materials (particles carried by the wind), air pollutants present in the form of chlorides and sulfates, and remnants of coatings. Notably, oxygen was present in all alteration layers and at higher concentrations than iron. This significant presence of oxygen indicates the formation of iron oxides and hydroxides, which are common iron corrosion products [19-21].

Uncorroded metallic substrate

Exclusively circular inclusions were identified in the unaltered iron matrix. These inclusions are not perfectly round and tend to appear moderately elongated, as observed in samples taken from the guardrails and pillars (Figure 5). This type of microstructure is characteristic of malleable or nodular (ductile) gray cast iron. Malleable cast iron is produced through heat treatments of white cast iron, which promote the formation of nodules. Nodular cast iron, on the other hand, is directly obtained during the casting process through the addition of inoculants that promote the nodular precipitation of graphite [16, 22].

The microstructure of both alloys is quite similar. However, some differences may arise from their manufacturing processes. The first factor is the cost: producing nodules during smelting and casting is less expensive than through heat treatments. Another factor is section limitation, as ductile iron can be produced in much larger sections compared to malleable iron [23-24]. Considering the need for efficiency and cost-effectiveness in historical prefabricated iron architecture, it is more plausible that the alloys studied are classified as nodular cast iron.

According to the chemical characterization of samples B1-A4, B2-A4, and B3-A3, the nodular precipitations are composed of elements other than iron: primarily carbon, manganese, silicon, oxygen, sulfur, and phosphorus. The isolated presence of aluminum and chlorine in samples B2-A4 and B4-A4 suggests contamination (*e.g.* from soil dust particles) and active corrosion in the alloy, leading to the formation of chlorides [15, 21] (Figure 6).

In samples 1D-A1 and B1-A4, areas (voids) with a different shape from the inclusions and a slightly darker gray color can be observed. However, there is no significant contrast in composition, as iron, carbon, oxygen, manganese, sulfur, and silicon were identified, almost entirely matching what was detected in the unaltered alloy and inclusions (Figure 6). This minimal variation can be attributed to the homogeneity in type, raw material of origin, and fabrication technology of the alloys.
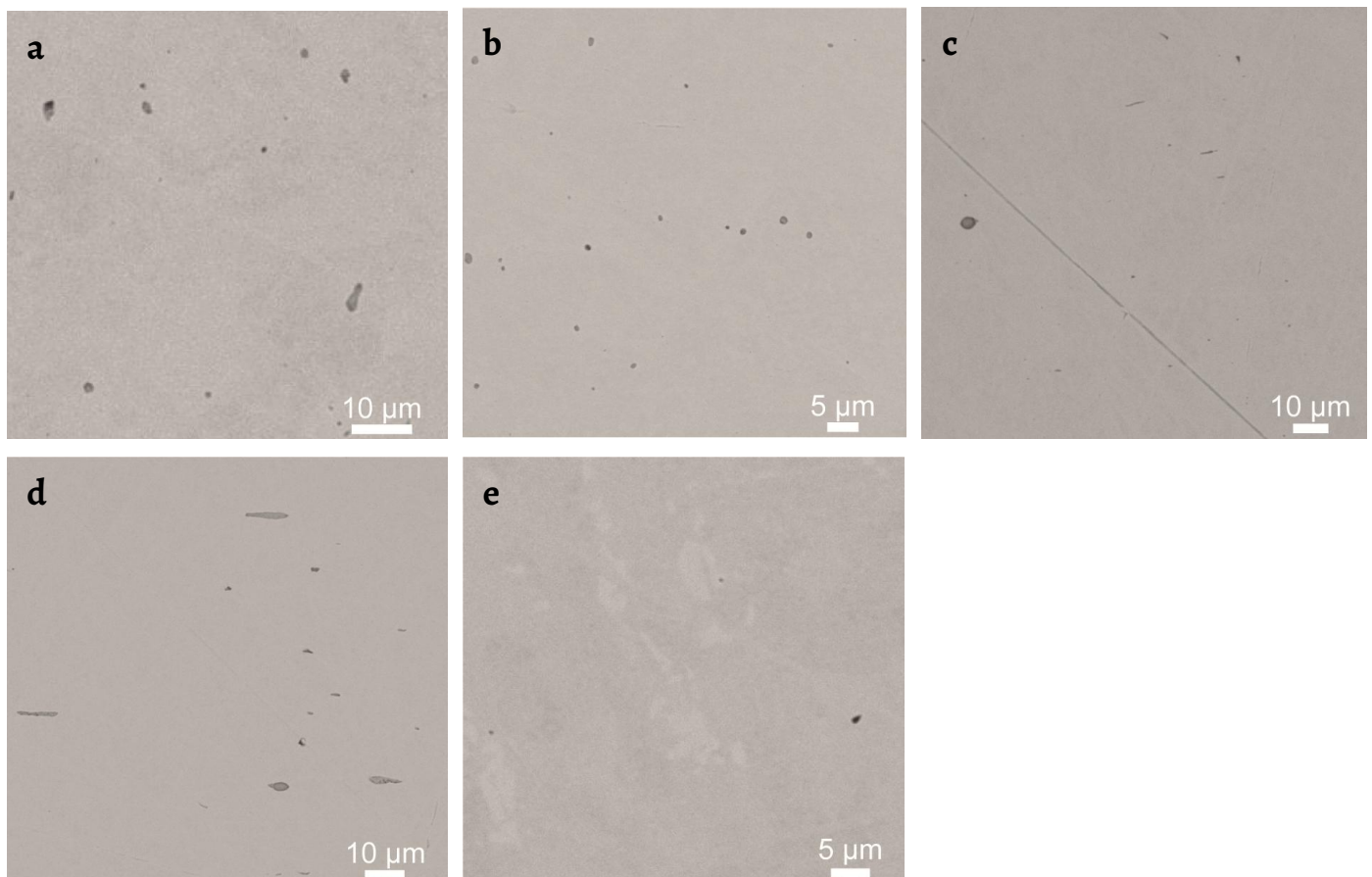

Figure 5. SEM images showing circular inclusions in the microstructure of the samples: *a)* 1D-A1; *b)* B1-A4; *c)* B2-A4; *d)* B3-A3; *e)* B4-A4.
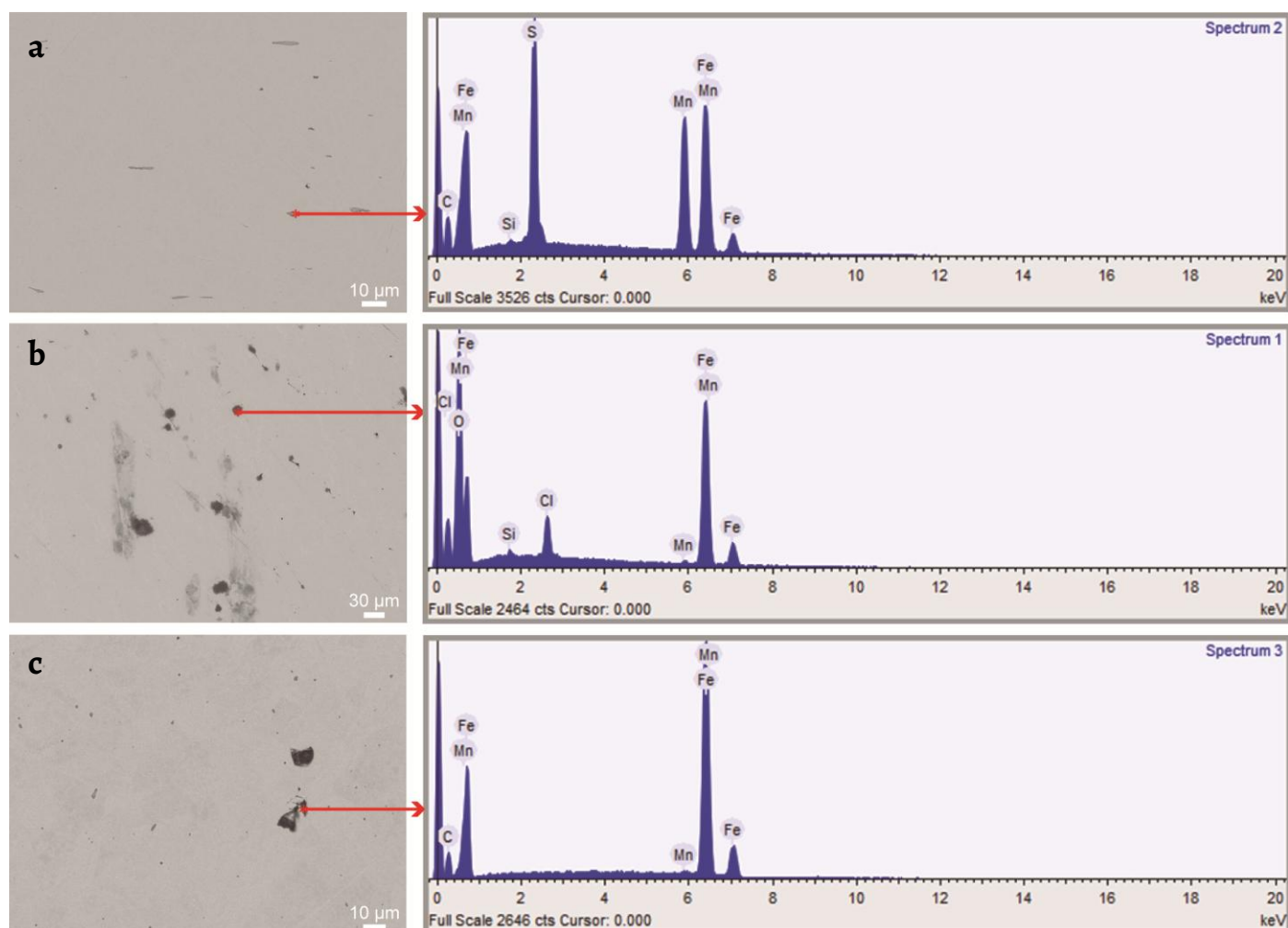
Figure 6. SEM images (left) and EDS spectra (right) showing: *a)* the chemical composition of the circular inclusions in sample B3-A3; *b)* the Cl identification in sample B4-A4; *c)* the chemical composition of the void areas in the sample 1D-A1.

One sample, 1D-A3, from a roof sheet, has a smooth texture and is free of inclusions. EDS analysis identified that the unaltered metal area is primarily composed of iron (Figure 7). In contrast, the XRD analysis of sample 1D-A4, taken from one of the faces of the same element as 1D-A3 and shown in Figure 4, indicates that the surface composition is zinc. The microstructure and zinc-rich surface composition were observed only on these roofing samples.

Although zinc is a typical metal for roofing in bandstands from the nineteenth and twentieth centuries [2], the contrasting chemical and mineralogical compositions suggest that it is an iron sheet coated with zinc. For an accurate determination of the ferrous alloy, the morphology and microstructure can be examined. According to the literature, lamellae and nodules are characteristics of gray cast iron; a fibrous texture formed by filamentous slags is typical of wrought iron; and the absence of these features distinguishes steel from the other types mentioned [22, 25-27]. Based on this information and the SEM images, it is reasonable to classify the 1D-A3 sample as a steel sheet.

Metallized steel sheet roofs have been used in historical architecture for centuries, similar to zinc coatings for metallic protection [28-29]. Concerning its function, the zinc coating on sample 1D-A4 acts as a protective mechanism for the base metal alloy (iron). It provides not only a protective barrier but also cathodic protection. In areas where the coating is defective and the iron is exposed, zinc serves as a sacrificial layer, corroding itself instead of the iron alloy [30].
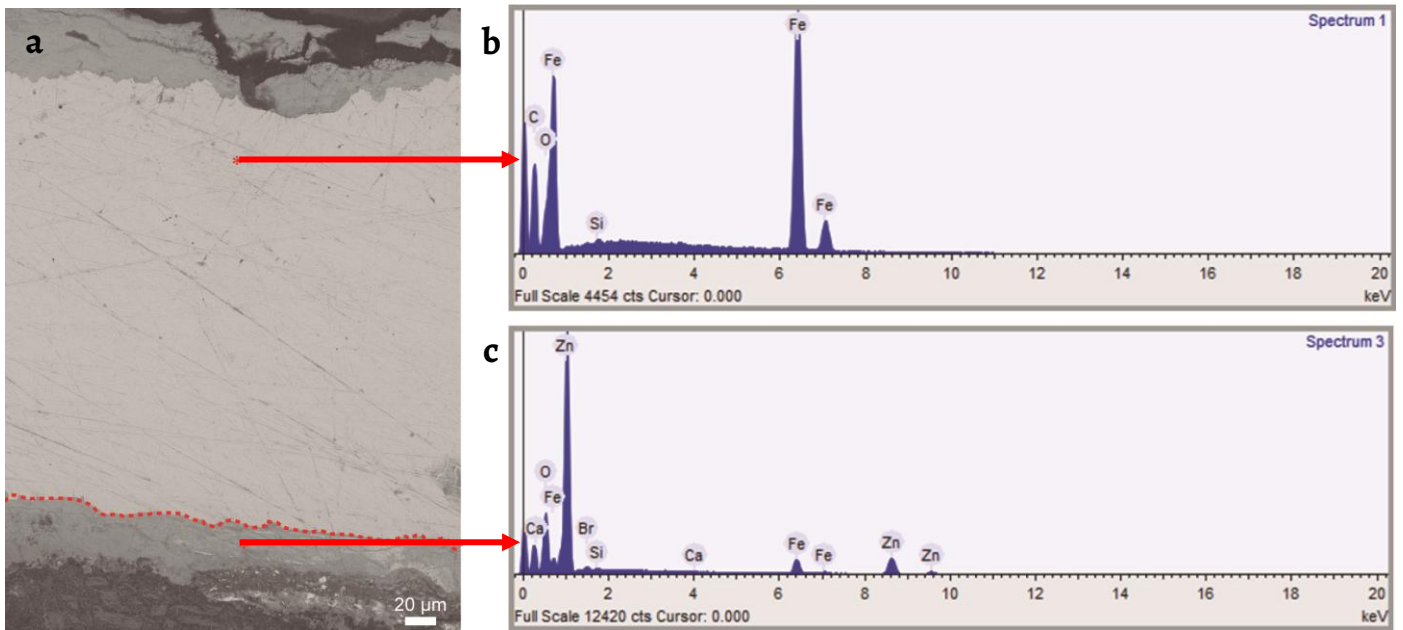
Figure 7. SEM image (left) and EDS spectra (right) of the roofing element showing: *a)* the absence of inclusions in sample 1D-A3; *b)* the alloy composition; *c)* the Zn coating in one of its faces.

Corrosion products

The samples investigated by using SEM/EDS included three groups of architectural elements: pillars, guardrails, and roof sheets. The images reveal a stratification consisting of unaltered metal, corrosion products, and coating remnants. In addition to chemical variations, coatings (paint or metallic) may be present or absent – as they, although recently renewed (2020/2021), were prone to loss due to the high chalking and dustiness of the parts.

Three sequences of layers were displayed: 1) uncorroded metal as the inner layer, followed by corrosion products intermediately, and paint as the outermost layer; 2) uncorroded metal as the inner layer and corrosion products as the outermost layer; 3) uncorroded metal intermediately and the corrosion product and zinc coating layers on the opposite faces of the element. Examples of the orders are shown in Figure 8.

In the Primeiro de Dezembro Pavilion, the position and composition of the corrosion products in samples 1D-A1 (guardrail) and 1D-A3 (roof sheet) differ. In sample 1D-A1, the corrosion appears as an intermediate layer, with the remaining paint as the outermost layer in 1D-A1. In contrast, in sample 1D-A3, the layers are not consecutive, as the zinc coating is present on only one face of the source object (Figure 8).

Sample 1D-A1 contained iron, carbon, oxygen, sodium, chlorine, calcium, potassium, and sulfur in its corrosion layer. Its paint layer was composed of iron, carbon, oxygen, manganese, silicon, sulfur, calcium, and chlorine. In the analysis of sample 1D-A3, the corrosion layer and zinc coating were found to consist of the following elements, respectively: iron, oxygen, and carbon in the corrosion layer; and zinc, oxygen, iron, bromine, silicon, and calcium in zinc coating. It should be highlighted that both compositions regard the iron substrate and metallic coating (Zn) corrosion.

In the other four bandstands, B1, B2, B3, and B4, only corrosion product layers were observed, in addition to the unaltered metal alloy. A notable feature is the extremely non-uniform thickness of the layers, along with high levels of fragmentation due to the advance of corrosion. The estimated thicknesses of the layers, measured by image proportion, varied between 15-30 μm in sample 1D-A1; 50-60 μm in sample 1D-A3; 10-17 μm in sample B1-A4; 20-30 μm in sample B2-A4; 10-60 μm in sample B3-A3; and 60-65 in sample B4-A4. The chemical elements detected were primarily iron, oxygen, and carbon with small amounts of silicon, calcium, sulfur, and manganese (Figure 9).
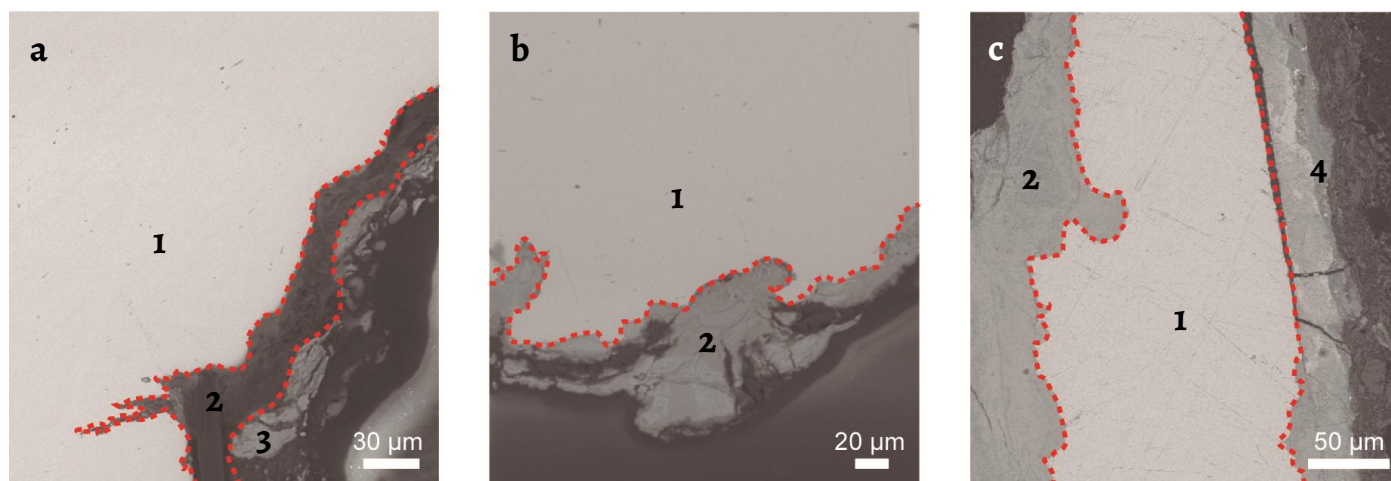
Figure 8. SEM images showing the stratigraphy of the layers in: *a)* sample 1D-A1; *b)* sample B3-A3; *c)* sample 1D-A3. 1 – uncorroded metal, 2 – corrosion product, 3 – paint, 4 – zinc coating.
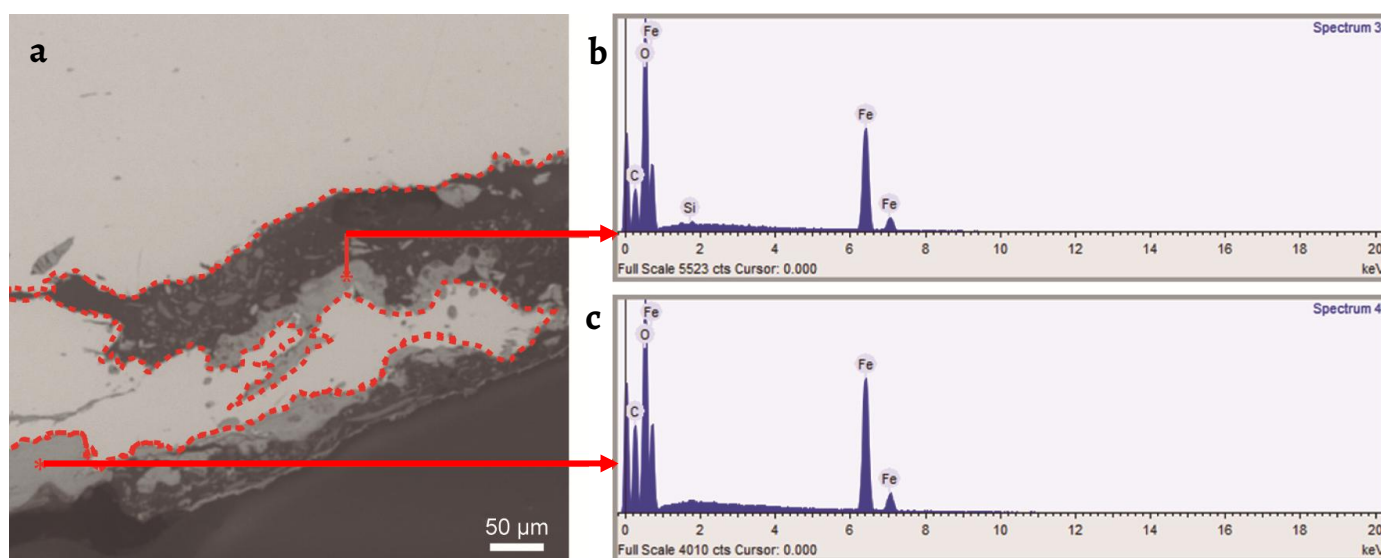

Figure 9. Sample B2-A4: *a)* SEM image showing the corrosion product layer thickness; *b-c)* EDS spectra of its chemical composition.

Regardless of the arrangement, it is evident that the layers are composed of elements common to cast iron alloys and other materials related to atmospheric pollutants, as previously mentioned. The presence of coating remnants (paint or metallic) is indicated by the detection of Zn in sample 1D-A3 and likely by the identification of Ca among other samples – possibly suggesting the presence of zincite (ZnO) and calcite ($CaCO_3$) from paints and primers applied to the surfaces of the bandstands [31].

Discussion

As anticipated based on the historical context of these buildings, the physical, chemical, and mineralogical characterization confirmed that the construction material is iron. However, the metallized steel sheet identified on the roof of the Primeiro de Dezembro Pavilion is likely a more recent addition or replacement. This inference is supported by documental alterations to the roofs of the music pavilions, as detailed in previous research [8, 32].

In addition to the buildings discussed in this article, circular inclusions were also found in the alloy used in another prefabricated structure from the same period, specifically in the characterization of the alloys of the Ver-o-Peso Iron Market, particularly in structural components [31]. The difference lies in the intended use of these inclusions, as nodules can

enhance the material's mechanical properties [33]. However, this may not have been a consideration for the structures studied, as the material was used both in load-bearing elements (pillars) and in parts with ornamental functions (guardrails).

In related studies, lamellae graphite is more commonly identified within the microstructure of iron building components, as observed in the case of the Iron Market and the United States Capitol Dome [31, 34]. Additional research on cast iron street furniture by Soffritti et al. [21, 35-36] supports this observation, revealing various types of lamellae graphite in specimens of English, Italian, and French origins. Despite the variety of microstructures reported in these studies, spheroidal graphite is not commonly or significantly present.

The significant presence of nodular cast iron in the five German structures studied, likely from a common manufacturer, raises questions about the iron industry technology in 1903 and its application in architecture. Literature suggests that efforts to improve cast iron properties through the addition of chemical elements like magnesium and cerium began in the 1930s, leading to the development, enhancement, and patenting of nodular cast iron around 1950 [24, 37-38].

It is important to note that neither magnesium nor cerium were detected in the EDS spectra of the samples. Additionally, the buildings' construction dates are inconsistent with the period during which this alloy first appear. Consequently, the initial classification of the metal is questionable. Therefore, the characteristics observed in the samples do not allow them to be accurately classified as either malleable or nodular/ductile cast iron, considering both the chemical properties and manufacturing practices valued at the time.

Further research is needed to clarify the typological definition of historical circular graphite ferrous alloys. Although the microstructure appears recent in metallurgical terms, ongoing studies on the formation of nodules suggest that the debate is still active [39]. Moreover, the results observed across this group of buildings and their different elements are unlikely to be coincidental. This indicates a potential for further development in metallurgical knowledge related to iron architecture, including insights into manufacturers, techniques, and variety of alloys used.

Few studies have been conducted on the Amazonian scenario regarding corrosion progression in similar buildings. Evidence of corrosion between unaltered metal and paint layers, a sign of poorly protected alloys, has been previously identified [31]. This may suggest a pattern of deterioration in the local architectural iron monuments that requires confirmation. Nonetheless, the effects of the equatorial hot and humid climate are thus more detailed in relation to other types of historical substrates (for example, glazed ceramic tiles) [40-41]. Therefore, investigations should be conducted to advance this specific understanding of the metallic heritage behavior.

The estimated thicknesses of the corrosion layers show that the alteration process may have resulted primarily from a couple of years of exposure (2020/2021). Literature measurements consider that 10-year-old layers are over 100 μm thick [19]. Iron metalworks from the same historical period, but in different environments and with more years of corrosion progression, have shown to be within this rate. In contrast, most of the dimensions observed in the samples were approximately 10 and 30 μm. According to the yearly rates of 25 μm/y for non-polluted atmospheres and 150 μm/y for polluted ones [21], the local process aligns with the conventional model of outdoor corrosion.

The corrosion stratification, consisting of a single layer in the samples, displayed less complexity compared to the more common two/three-layered cases. The appearance of the samples indicates that they are porous and nonprotective. Their visual features also suggest no graphitic corrosion traces in terms of morphology. This specific form of cast iron corrosion, which is attributed to mild atmospheres and acidic precipitation, has been identified in European structures. This causes mechanical weakening of the material while preserving its shape [19, 21, 42]. From this perspective, the concerns involving the bandstands' conservation may not include sudden structural failure.

This context inevitably highlights their surface protection situation. Based on the investigation, there are no substantial corrosion differences compared to other structures and environmental conditions. However, the coatings could be an issue, as it has demonstrated a very short service life. These findings corroborate previous studies that pointed out irregular maintenance of the protective systems used in the restoration of the bandstands over the years [32]. The regular deterioration of organic coatings and potential regional challenges regarding the durability of surface treatments must be verified.

Conclusion

Part of the world's historical and architectural legacy from a century ago, Belém's German bandstands accrued significant heritage value and meaning. However, inadequate knowledge has impacted on their conservation and preservation, leading to advanced alteration processes, architectural disfigurement, and poorly scientifically grounded maintenances. For a better developed scientific knowledge and conservation practice, this study produced data on their metal alloys and corrosion products' physical (texture, thickness, and alloy microstructure), chemical, and mineralogical characteristics (mineral phases of the alloys).

The application of analytical techniques successfully provided technological data about these constructions. The analysis confirmed that iron is the primary material used, with a significant presence of nodular gray cast iron. This information is valuable for planning future restorations, particularly for the repair and replacement of components. Moreover, the observed microstructure highlights the expertise and practices employed by European foundries, mainly German.

Regarding the alteration processes, the results indicated that there are no significant differences in corrosion levels when compared to other structures and environmental conditions. Nevertheless, it showed that the corrosion on these buildings could be directly related to their coatings' rapid decrease in protection capacity. This highlights a concern: the bandstands, which underwent recent restorations in 2020-2021, are not receiving appropriate treatments. Accordingly, corrosion and coating behavior should be evaluated and inserted in the Amazonian weathering factors – extreme humidity, temperature, and rainfall – to further support these conclusions.

It remains valuable to collect and analyze samples from other construction parts. Such analysis would provide better opportunities to identify the alloys and materials used and assess the compatibility of past treatments. Additionally, given the unique characteristics observed, there is a need to develop a comparative study of German historical alloys. This is particularly important due to the scarcity of data on similar building materials from the early industrialization period and the same origin for contrasting information.

Subsequent steps should include testing ironwork material based on the composition of the historical material. This involves experimenting with methods for repairing or replacing parts and joining new metals with the original ones to prevent issues such as bi-metallic corrosion, structural failure, and excessive disposal of components. Additionally, testing the efficiency and durability of protective systems components, such as paints, under representative Amazonian conditions is essential. This approach, combined with critical theoretical thinking, would aid in developing conservation guidelines and provide insights into the preservation of metallic industrial heritage as a whole.

REFERENCES

1. Lister, R., *Decorative cast ironwork in Great Britain*, G. Bell and Sons, London, (1960).

2. Silva, G. G. da, *Arquitetura do ferro no Brasil*, Nobel, São Paulo (1986).

3. Higgs, M., 'The exported iron buildings of Andrew Handyside & Co. of Derby', *Journal of the Society of Architectural Historians* **29**(2) (1970) 175-180, https://doi.org/10.2307/988651.

4. Gomes, G., 'Artistic intentions in iron architecture', *The Journal of Decorative and Propaganda Arts* **21** (1995) 86-107, https://doi.org/10.2307/1504133.

5. Sarges, M. N., *Belém: riquezas produzindo a belle époque (1870-1912)*, 3rd ed., Editora Paka-Tatu, Belém (2010).

6. Coelho, G. M., 'Belém e a belle époque da borracha', *Revista Observatório* **2**(5) (2016) 32-56, https://doi.org/10.20873/uft.2447-4266.2016v2n5p32.

7. Lemos, A. J. de, 'O município de Belém. Relatório apresentado ao Conselho Municipal de Belém capital do Pará referente à 1903', s.n., Belém (1904), https://obrasraras.fcp.pa.gov.br/publication/file/relatorios/lemos/omunicipiodebelemrelatoriolemos1904referentea1903/ (accessed 2023-10-06).

8. Oliveira, T. T. S.; Palácios, F. O., 'History and architectural characteristics of the iron bandstands in Belém, Pará', *PARC Pesquisa em Arquitetura e Construção* **14** (2023) e023016, https://doi.org/10.20396/parc.v14i00.8670968.

9. Sembrat, J.; Rabinowitz, M.; Bello, J., 'Investigating and restoring decorative finishes on architectural metals', *Journal of Architectural Conservation* **18**(3) (2012) 27-51, https://doi.org/10.1080/13556207.2012.10785117.

10. de Bouw, M.; Wouters, I.; Vereecken, J.; Lauriks, L., 'Iron and steel varieties in building industry between 1860 and 1914 – a complex and confusing situation resolved, *Construction and Building Materials* **23**(8) (2009) 2775-2787, https://doi.org/10.1016/j.conbuildmat.2009.03.009.

11. de Ruggiero, A. C; Calzolari, L.; Soffritti, C.; Varone, A., Garagnani, G. L., 'Cast iron metalworks in European urban furniture dating back to the 19th and the early 20th centuries', *Materials Science Forum* **941** (2018) 663-667, https://doi.org/10.4028/www.scientific.net/MSF.941.663.

12. Scott, D. A., 'The use of metallographic and metallurgical investigation methods in the preservation of metallic heritage artefacts', in Corrosion *and Conservation of Cultural Heritage Metallic Artefact*, eds. P. Dillmann, D. Watkinson, E. Angelini and A. Adriaens, Woodhead Publishing, Cambridge (2013) 1-5, https://doi.org/10.1533/9781782421573.2.82.

13. Dillmann, P.; Watkinson, D.; Angelini, E., Adriaens, A., 'Introduction: conservation versus laboratory investigation in the preservation of metallic heritage artefacts, in *Corrosion and Conservation of Cultural Heritage Metallic Artefacts*, eds. P. Dillmann, D. Watkinson, E. Angelini and A. Adriaens, Woodhead Publishing, Cambridge (2013) 82-99, https://doi.org/10.1533/9781782421573.1.

14. Goldstein, J. I.; Newbury, D.E.; Michael, J. R.; Ritchie, N. W. M.; Scott, J. H. J.; Joy, D. C., 'SEM image interpretation', in *Scanning Electron Microscopy and X-Ray Microanalysis*, eds. J. I. Goldstein, D. E. Newbury, J. R. Michael, N. W. M. Ritchie, J. H. J. Scott and D. C. Joy, Springer, New York (2018) 111-121, https://doi.org/10.1007/978-1-4939-6676-9_7.

15. Gimeno Adelantado, J. V.; Ferrer Eres, M. A.; Valle Algarra, F. M.; Peris Vicente, J.; Bosch Reig, F., 'Analytical study by SEM/EDX and metallographic techniques of materials used in the iron production process during the Iberian period', *Talanta* **60**(5) (2003) 895-910, https://doi.org/10.1016/S0039-9140(03)00152-8.

16. Colpaert, H., *Metalografia dos Produtos Siderúrgicos Comuns*, Blucher, São Paulo (2008).

17. Singhal, P.; Saxena, K. K., 'Effect of silicon addition on microstructure and mechanical properties of grey cast iron: an overview', *Materials Today: Proceedings* **26** (2020) 1393-1401, https://doi.org/10.1016/j.matpr.2020.02.281.

18. Srivastava, R.; Singh, B.; Saxena, K. K., 'Influence of S and Mn on mechanical properties and microstructure of grey cast iron: an overview', *Materials Today: Proceedings* **26** (2020) 2770-2775, https://doi.org/10.1016/j.matpr.2020.02.577.

19. Hœrlé, S.; Mazaudier, F., Dillmann, P. H.; Santarini, G., 'Advances in understanding atmospheric corrosion of iron. II. Mechanistic modelling of wet–dry cycles', *Corrosion Science* **46**(6) (2004) 1431-1465, https://doi.org/10.1016/j.corsci.2003.09.028.

20. Kreislova, K.; Knotkova, D.; Geiplova, H., 'Atmospheric corrosion of historical industrial structures', in *Corrosion and Conservation of Cultural Heritage Metallic Artefacts*, eds. P. Dillmann, D. Watkinson, E. Angelini and A. Adriaens, Woodhead Publishing, Cambridge (2013) 311-343, https://doi.org/10.1533/9781782421573.3.311.

21. Soffritti, C.; Calzolari, L.; Balbo, A.; Zanotto, F.; Monticelli, C.; Ospitali, A.; Garagnani, G. L., 'Conservation state of cast iron metalworks in European street furniture', *The European Physical Journal Plus* **134**(9) (2019) 424, https://doi.org/10.1140/epjp/i2019-12944-y.

22. Durand-Charre, M., *Microstructure of steels and cast irons*, Springer Berlin, Heidelberg, (2004), https://doi.org/10.1007/978-3-662-08729-9.

23. Rundman, K. D.; Iacoviello, F., 'Cast irons', in Cast irons, in *Reference Module in Materials Science and Materials Engineering*, Elsevier, Oxford (2016) 1003-1010, https://doi.org/10.1016/B978-0-12-803581-8.09803-9.

24. Iacoviello, F.; di Cocco, V.; Favaro, G., 'Pearlitic ductile cast iron: mechanical properties gradient analysis in graphite elements', *Procedia Structural Integrity* **9** (2018) 9-15, https://doi.org/10.1016/j.prostr.2018.06.004.

25. Walker, R., 'The production, microstructure, and properties of wrought iron', *Journal of Chemical Education* **79** (2002) 443, https://doi.org/10.1021/ed079p443.

26. O'Sullivan, M.; Swailes, T., 'A study of historical test data for better informed assessment of wrought iron structures', *International Journal of Architectural Heritage* **3**(4) (2009) 260-275, https://doi.org/10.1080/15583050902802337.

27. di Lorenzo, G.; Formisano, A.; Terracciano, G., Landolfo, R., 'Iron alloys and structural steels from XIX century until today: evolution of mechanical properties and proposal of a rapid identification method', *Construction and Building Materials* **302** (2021) 124132, https://doi.org/10.1016/j.conbuildmat.2021.124132.

28. Källbom, Arja; Almevik, Gunnar, 'Maintenance of painted steel-sheet roofs on historical buildings in Sweden', *International Journal of Architectural Heritage* **16**(4) (2022) 538-552, https://doi.org/10.1080/15583058.2020.1808910.

29. Gerengi, Husnu; Solomon, Moses M.; Maraslı, Muhammed; Kohen, Beni B., 'A comparative analysis of the corrosion characteristics of electro-galvanized steel coated with epoxy zinc-free and zinc-rich coatings in 5 % NaCl', *Journal of Adhesion Science and Technology* **37**(20) (2023) 2795-2806, https://doi.org/10.1080/01694243.2022.2123603.

30. Torraca, G., *Lectures on materials science for architectural conservation*, The Getty Conservation Institute, Los Angeles (2009).

31. Palácios, F. O.; Angélica, R. S.; Sanjad, T. A. B. C., 'The metal alloys from the XIX century and weathering action in the Mercado do Ver-o-Peso building, northern Brazil: identification with the usage of laboratory analysis', *Materials Characterization* **96** (2014), 225-233, https://doi.org/10.1016/j.matchar.2014.08.004.

32. Oliveira, T. T. S.; Palácios, F. O., 'Os coretos de ferro dos séculos XIX e XX em Belém (PA): transformações e reconhecimento de significados e valores', *Revista CPC* **18**(35) (2023) 140-172, https://doi.org/10.11606/issn.1980-4466.v18i35p140-172.

33. Tewary, U.; Paul, D.; Mehtani, H. K.; Bhagavath, S.; Alankar, A.; Mohapatra, G.; Sahay, S. S.; Panwar, A. S.; Karagadde, S.; Samajdar, I., 'The origin of graphite morphology in cast iron', *Acta Materialia* **226** (2022) 117660, https://doi.org/10.1016/j.actamat.2022.117660.

34. McCowan, C. N.; Siewert, T. A.; McColskey, J. D.; Hildebrand, K.; Olson, D. L., 'United States Capitol dome: characterization of cast and wrought materials', *Materials Characterization* **62** (2011) 807-816, https://doi.org/10.1016/j.matchar.2011.05.002.

35. Soffritti, C.; Calzolari, L.; Balbo, A.; Zanotto, F.; Monticelli, C.; Fortini, A.; Garagnani, G. L., 'Study of the conservation state of European street furniture in painted cast irons', La *Metallurgia Italiana* **4** (2018) 5-16, http://www.aimnet.it/la_metallurgia_italiana/2018/aprile/soffritti.pdf (accessed 2022-12-15).

36. Soffritti, C.; Calzolari, L.; Pepi, S.; Fortini, A.; Merlin, M.; Garagnani, G. L., 'Metallurgical and statistical approaches to the study of cast iron street furniture', *Metallurgical and Materials Transactions A* **52** (2021) 1127-1141, https://doi.org/10.1007/s11661-021-06135-6.

37. Stefanescu, D. M., 'A history of cast iron', in *Handbook ASM. Volume 1A – Cast iron science and technology*, ed. D. M. Stefanescu, ASM International, Ohio (2017) 3-11, https://doi.org/10.31399/asm.hb.v01a.a0006320.

38. Bramaramba, V.; Behera, R. K.; Saurabh, S.; Sen, S., 'Quantitative phase analysis: it's role in characterization of spheroidal graphite iron', *Materials Today: Proceedings* **27** (2020) 1728-1732, https://doi.org/10.1016/j.matpr.2020.03.649.

39. Lacaze, J.; Connétable, D., Castro-Román, M. J., 'Effects of impurities on graphite shape during solidification of spheroidal graphite cast irons', *Materialia* **8** (2019) 100471, https://doi.org/10.1016/j.mtla.2019.100471.

40. Costa, Marcondes L. da; Sanjad, Thais A. B. C.; Paiva, Rosildo S., 'The mineralogy and chemistry of the German and Portuguese tiles used to face a historic building in the Amazon region and their natural susceptibility to tropical weathering', *Acta Amazonica* **43**(3) (2013) 323-330, https://doi.org/10.1590/S0044-59672013000300008.

41. Sanjad, Thais A.B.C.; Costa, Marcondes L. da; Paiva, Rosildo S.; Palácios, Flávia Olegário, 'Ação microbiológica nos azulejos históricos das fachadas de Belém, região amazônica', *PÓS: Revista do Programa de Pós-graduação em Artes da EBA/UFMG* **4**(8) (2014) 124-133, https://periodicos.ufmg.br/index.php/revistapos/article/view/15484.

42. Sykora, Miroslav; Kreislova, Katerina; Pokorny, Petr, 'Corrosion of historic grey cast irons: indicative rates, significance, and protection', *International Journal of Computational Methods and Experimental Measurements* **8**(2) (2020) 162-174, https://doi.org/10.2495/CMEM-V8-N2-162-174.